Eur. Phys. J. A (2022) 58:11
https://doi.org/10.1140/epja/s10050-022-00663-4

THE EUROPEAN PHYSICAL JOURNAL A

Regular Article - Experimental Physics

Alpha-gamma decay studies of ^{247}Md

F. P. Heßberger[1,2,a], S. Antalic[3], F. Giacoppo[1], B. Andel[3], D. Ackermann[1,6], M. Block[1,2,4], S. Heinz[1], J. Khuyagbaatar[1], I. Kojouharov[1], M. Venhart[5]

[1] GSI-Helmholtzzentrum für Schwerionenforschung GmbH, 64291 Darmstadt, Germany
[2] Helmholtz Institut Mainz, 55099 Mainz, Germany
[3] Department of Nuclear Physics and Biophysics, Comenius University in Bratislava, 84248 Bratislava, Slovakia
[4] Johannes Gutenberg-Universität Mainz, 55128 Mainz, Germany
[5] Institute of Physics, Slovak Academy of Science, 84511 Bratislava, Slovakia
[6] *Present address:* GANIL, 14076 Caen, France

Received: 15 September 2021 / Accepted: 22 December 2021 / Published online: 25 January 2022

Communicated by A. Kankainen

Abstract Alpha decay and spontaneous fission of the ground-state and the isomeric state of ^{247}Md were investigated with specific emphasis to identify the ground-state of the daughter nucleus ^{243}Es. The decay studies were accompanied by measuring α-γ coincidences. On the basis of the measured data an improved decay scheme of ^{247}Md is proposed. Spontaneous fission half-lives of ^{247g}Md and ^{247m}Md were determined and the fission hindrance of the high spin ground-state ($7/2^-$) relative to the low spin isomeric state ($1/2^-$) was estimated.

1 Introduction

Superheavy nuclei owe their stability against spontaneous fission due to shell effects [1]. Therefore evaluation of their shell structure is decisive for understanding their existence, and provides also a stringent test for theoretical models describing nuclear properties. One strategy to do so is to investigate systematic trends in single-particle levels ('Nilsson levels') in deformed nuclei. As the unpaired nucleon essentially acts as a spectator when a pair of protons or neutrons is added to the nucleus, at low excitation energies odd-mass even-Z nuclei exhibit a similar structure along the isotone lines (N=const.), while odd-mass odd-Z nuclei exhibit a similar structure along the isotope lines (Z=const.) (see e.g. Refs. [2,3] for more detailed discussions).

At present, mendelevium (Z=101) is the heaviest odd-Z element for which such systematic studies have been performed over a wide range of isotopes (A=247–257) [5]. The ground-state of the odd-mass mendelevium isotopes is assigned as $7/2^-$[514] [4–6]. It was found that this state essentially decays into the corresponding state in the einsteinium daughter nuclei, which then decays by E1 transitions into the $7/2^+$[633] Nilsson level or the $9/2^+$ member of the rotational band built on it. But this Nilsson level is not necessarily the ground-state. Indeed it was assigned as the ground-state in ^{249,253}Es [7,8], while in ^{251}Es the ground-state was assigned as $3/2^-$[521] [4]. For the lighter einsteinium isotopes the situation is unclear, as one can assume from the properties of the heavier ones, that the $3/2^-$[521] and $7/2^+$[633] levels may lie close in energy and alternate as ground-state. More detailed investigations of these isotopes are necessary. As in a recent investigation of ^{247}Md [9] this problem was not solved, another study was performed.

Originally, ^{247}Md was discovered in an irradiation of ^{209}Bi with ^{40}Ar at SHIP [10] and identified by α-α-correlations to its known daughter product ^{243}Es. In an experiment at SHIP in 1993 the α decay data were improved (E_α = 8424 keV, $T_{1/2}$ = 1.12 ± 0.22 s). Also another state of $T_{1/2} = 0.23^{+0.18}_{-0.12}$ s decaying by spontaneous fission was identified [11]. It was tentatively assigned as the $1/2^-$[521] ground-state, while the α activity was assigned to an isomeric state of $7/2^+$[633] or $7/2^-$[514] configuration.

In a later study [9] at SHIP also α decay of E_α = 8783 ± 40 keV (and a tentative line E_α = 8616 ± 20 keV) was observed for the activity of shorter half-life. However, based on the decay properties (specifically α-γ coincidences) of the 1.2-s activity similar to that of other investigated odd-mass mendelevium isotopes the latter was assigned as to the ground-state with $7/2^-$[514] configuration [5,9], while the 0.23-s activity was assigned to an isomeric state of $1/2^-$[521] configuration. To obtain more information about the decay of this level was another motivation for the present study.

[a] e-mail: F.P.Hessberger@gsi.de (corresponding author)

2 Experiment

The experiment was performed at GSI Darmstadt. The beam of $^{40}Ar^{10+}$ was delivered from the Penning source of the UNILAC. The targets were prepared from $^{209}Bi_2O_3$. Layers of ≈(450–490) μg/cm^2 (bismuth content ≈(390–420) μg/cm^2) were evaporated on-to carbon foils of ≈40 μg/cm^2 (upstream) and covered by a ≈10 μg/cm^2 carbon layer (downstream) to improve radiative cooling and to prevent sputtering of material out of the foils. The targets were mounted on a wheel which rotated synchronously to the beam macro structure (5 ms wide pulses at 50 Hz repetition frequency). The targets were irradiated at two beam energies E_{lab} = 186.4 MeV (beam dose 1.25×10^{18} projectiles) and E_{lab} = 188.0 MeV (beam dose 3.60×10^{18} projectiles). The beam intensity was up to 2000 *p*nA (1.24×10^{13} particles/s) at E_{lab} = 186.4 MeV. It was lowered to 1400–1500 pnA ((8.7–9.3)$\times 10^{12}$ particles/s) at E_{lab} = 188 MeV to reduce deterioration of the targets.

The evaporation residues (ER) leaving the targets with energies of around 40 MeV were separated from the primary beam by the velocity filter SHIP [12]. In the focal plane of SHIP, they were subsequently implanted into a position-sensitive 16-strip Si PIPS detector (stop detector) with an active area of 80 × 35 mm^2. It was used for measuring time, position, and kinetic energy of the residues as well as subsequent α decays or spontaneous-fission (SF) events [13]. The energy resolution of the detector system was $\Delta E = 30$ keV (FWHM). The detector strips were position sensitive in the vertical direction by charge division. For each strip two position signals were recorded, one relative to the top and one relative to the bottom of the strip. To measure α particles and fission fragments escaping the stop detector into the backward hemisphere, the latter was surrounded by a box consisting of six Si-wafers having shapes and sizes equal to that of the stop detector. They covered a solid angle of 85% of 2π.

Gamma rays were measured using a Ge-clover detector consisting of four crystals, each of (50–55) mm diameter and 70 mm length, which were shaped and assembled to form a block of 102 × 102 × 70 mm^3. The average γ rate (sum of all four clover segments) in coincidence with particles[1] was ≈20/s during the beam-off period and ≈80/s during the beam-on period. The clover-detector signals were recorded within a 5 μs coincidence window with particle registration in the stop detector or in one of the box detectors. Energy resolutions of 1.13 keV (FWHM), 1.24 keV (FWHM) and 1.7 keV (FWHM) were obtained for the E= 118.1 keV ($K_{\alpha 1}$(Es)), 157.1 keV and 209.6 keV transitions.

[1] α particles, spontaneous fission events, implanted nuclei (scattered projectiles, evaporation residues, products from few nucleons transfer), conversion electrons (CE) from electron capture (EC) decay. CE-γ coincidences stem from EC decay of nuclei produced in few nucleons transfer and their decay products and from decay of long-lived decay products of activities produced in previous experiments.

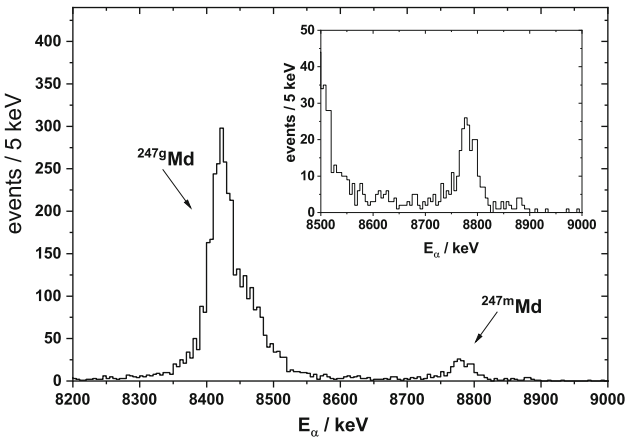

Fig. 1 Spectrum of α particles observed with full energy release in the stop detector between the beam bursts from the irradiations of ^{209}Bi with ^{40}Ar; the inset shows an expanded region of 8500–9000 keV

Further details are found in [14]. The corresponding irradiations were performed within the same beamtime campaign using exactly the same experimental set-up.

Theoretical α-decay half-lives are calculated using the semi-empirical formula presented by Poenaru et al. [15] using the parameter modification suggested by Rurarz [16]. This formula has been proven to reproduce α half-lives in the region of the heaviest nuclei within a factor of two [17].

The Q_α value is given by $Q_\alpha = (1+(m_\alpha/m_d)) \times E_\alpha$, with m_α representing the mass of the α particle and m_d representing the mass of the daughter nucleus, and $Q = Q_\alpha + E_\gamma$.

3 Experimental results

3.1 α decay and spontaneous fission (SF) events

The spectrum of α decays observed in the present study within the 15 ms beam-off period ('pause') between the 5 ms-beam bursts is shown in Fig. 1. In a first step events in the range E_α = (8350–8650) keV are attributed to the decay of the ground-state ^{247g}Md, those in the range E_α = (8700–8830) keV are attributed to the decay of the isomer ^{247m}Md on the basis of the results of the previous study [9]. The enery range E_α = (8650–8700) keV was not considered because of possibly containing events of both activities. The time distributions for both components are shown in Fig. 2a–d). From fitting expontial decay curves we obtained values $T_{1/2}$ = 1.20 ± 0.12 s for the component attributed to the ground-state, and $T_{1/2}$ = 0.23 ± 0.03 s for the component attributed to the isomer. For the 1.2 s-activity background became critical for long correlation times as seen specifically in Fig. 2b). So a constant background of

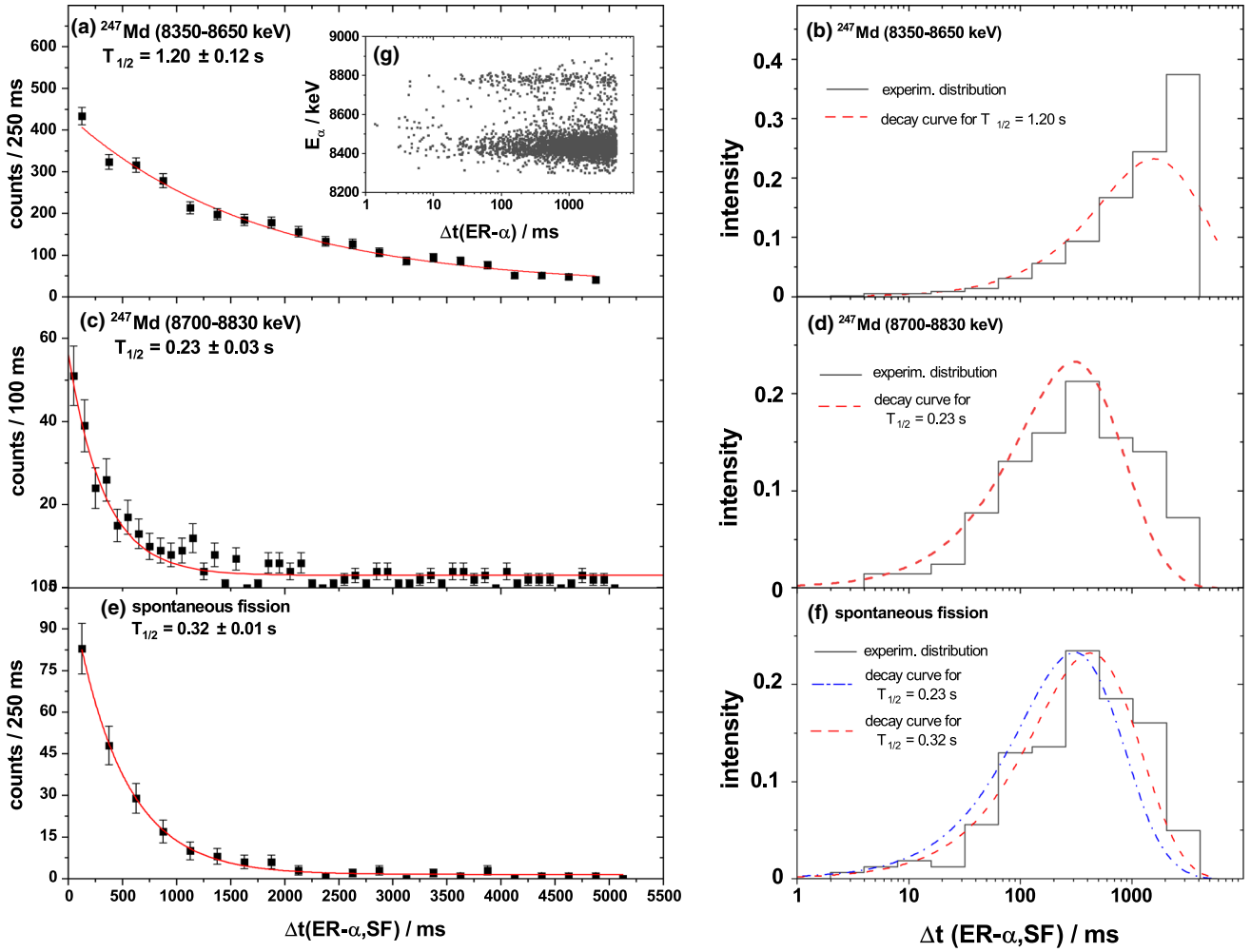

Fig. 2 Time distributions of α- and fission events observed in the irradiation of ^{209}Bi with ^{40}Ar; **a**, **b** α decay-events E_α = (8350–8650) keV in linear (**a**) and logarithmic (**b**) time scale, **c**, **d** α-events E_α = (8700–8830) keV, in linear (**c**) and logarithmic (**d**) time scale, **e**, **f** spontaneous fission events in linear (**e**) and logarithmic (**f**) time scale, **g** two dimensional plot correration times Δt(ER-α) versus E_α

25 events/time bin was considered in the fitting procedure. Besides α decays, 227 SF-events correlated to evaporation residues were observed. Their time distribution is shown in Fig. 2c, d). The extracted half-life is $T_{1/2} = 0.32 \pm 0.01$ s. Evidently the half-lives of the α-events attributed to the decay of the isomer and the SF events disagree. As the latter is longer than that of the α decays we assume that the fission events represent a mixture of SF from the ground-state and from the isomer. Hence the time distribution of the SF can be written as a function

$$f(t) = A \times exp(-ln2 \times t/T_{1/2}(^{247m}Md)) + B \times exp(-ln2 \times t/T_{1/2}(^{247g}Md))$$

The best agreement with the observed time distribution of all fission events is obtained with intensity ratios $I(^{247g}\text{Md})/I(\text{tot}) \approx 0.3$ and $I(^{247m}\text{Md})/I(\text{tot}) \approx 0.7$. With the numbers of α particles registered, respecting different detection efficiencies for α particles and SF we obtained $b_{sf} = 0.0086 \pm 0.0010$ for ^{247g}Md and $b_{sf} = 0.20 \pm 0.02$ for ^{247m}Md and hence spontaneous fission half-lives of $T_{sf} \approx 140$ s and $T_{sf} \approx 1.2$ s for ^{247g}Md and ^{247m}Md, respectively.

3.2 α-γ-measurements of ^{247}Md

The spectrum of γ rays observed in coincidence with α decays are shown in Fig. 3a–c). Besides the strong γ transitions at $E_\gamma = 209.6 \pm 0.1$ keV and $E_\gamma = 157.1 \pm 0.1$ keV, reported already earlier [5] and attributed to the transitions $7/2^-[514] \rightarrow 7/2^+[633]$, $7/2^-[514] \rightarrow 9/2^+$, and the $K_{\alpha 1,\alpha 2,\beta 1}$ X-ray lines of einsteinium (112.5 ± 0.2, 118.1 ± 0.1, 133.0 ± 0.1 keV) a couple of less intense transitions

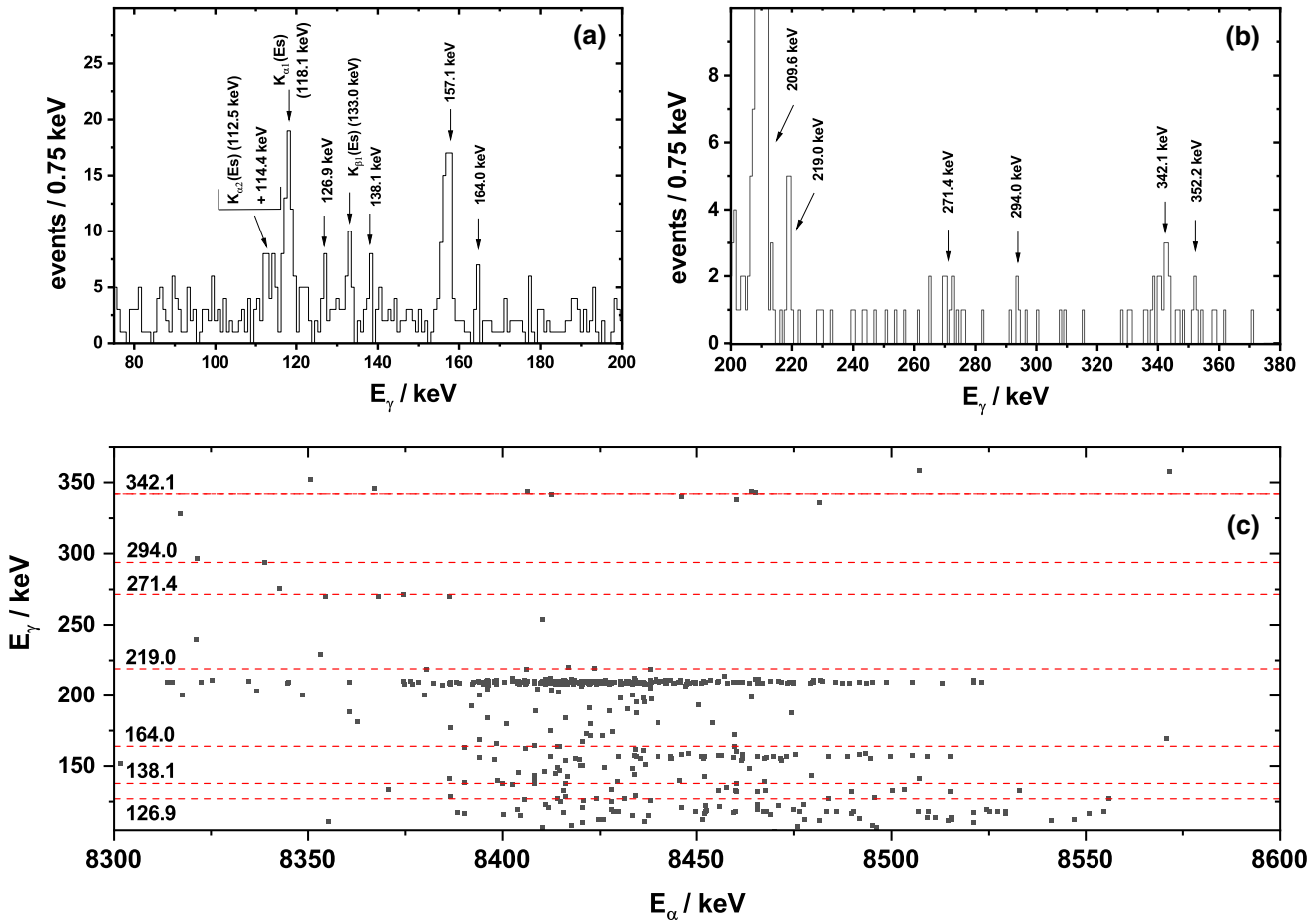

Fig. 3 Spectrum of γ events observed in coincidence with α-decays in the range $E_\alpha = (8300–8900)$ keV; for better presentation the spectrum has been split in two parts, **a** $E_\gamma = (50–200)$ keV, **b** $E_\gamma = (200–400)$ keV. To enhance statistics also the data from the previous study [9] were included. **c** Two dimensional plot of α energies versus γ energies. Due to worse energy resolution of α paricles registered as sum events in the stop and box detectors ($\Delta E_{stop} + E_{residual,bosx}$) only α events with full energy release in the stop detector are considered in this plot

Table 1 Observed numbers and half-lives of α- and fission events; the numbers of α-decays represent the events registered with full energy release in the stop detector between the beam bursts, the number of SF events represents those correlated to evaporation residues (ER) within $\Delta t = 5$ s

Decay mode	E_α/keV	Number of events	Half-life/s
α	8350–8650	3428	1.20 ± 0.12
α	8650–8900	299	0.23 ± 0.03
SF		227	0.32 ± 0.01

are observed. The prominent ones are $E_\gamma = 114.4 \pm 0.1$, 126.9 ± 0.5, 138.1 ± 0.3, 164.0 ± 0.7, 219.0 ± 0.1, 271.4 ± 1.5, 294.0 ± 0.3, 342.1 ± 1.3, and 352.2 ± 0.7 keV. The properties of these γ transitions will be discussed in the following and they will be placed in a decay scheme of ^{247g,247m}Md giving rise to a partial level scheme of ^{243}Es. The γ energies, energies of coincident α particles, and half-lives of the corresponding transitions, if evaluated, are given in Table 2. As seen from Fig. 3a a couple of more lines, specifically in the range $E_\gamma = 75–90$ keV, seem to be present. However, as it seems presently not possible to place them in a level scheme we will omit a discussion here. We will also not discuss further the lines at $E_\gamma = 209.6$ and 157.1 keV, as they have been assigned already in the previous publications [5,9].

K X-ray lines As seen from Fig. 3a the energy distribution of the γ events in the range $E_\gamma = (110.2–115.5)$ keV is quite broad. Fitting it with a single line one obtains $E_\gamma = 113.4 \pm 0.2$ keV, which differs from the $K_{\alpha 2}$ energy of einsteinium (112.53 keV [18]) by 0.9 keV. The line width of 3.8 keV (FWHM) is more than three times of the value 1.13 keV (FWHM) we obtain for the $K_{\alpha 1}$ line (118.1 keV) or 1.24 keV for the $E_\gamma = 157.1$ keV transition. So it is natural to assume this distribution as a line doublet. We obtained energies of $E_1 = 112.5 \pm 0.2$ keV and $E_2 = 114.4 \pm 0.1$ keV from fitting two Gaussians. However, then the corresponding intensity ratio is $I_{K\alpha 1}/I_{K\alpha 2} = 0.29 \pm 0.11$ which is only about half

Table 2 Assigned γ lines observed in coincidence with α decays of ^{247}Md

E_γ/keV	E_α/keV	Q/keV	$T_{1/2}$/s
112.5 ± 0.2 ($K_{\alpha 2}$(Es))	–	–	–
114.4 ± 0.1	8404–8644	–	$1.87^{+0.72}_{-0.40}$
118.1 ± 0.1 ($K_{\alpha 1}$(Es))	–	–	–
126.9 ± 0.5	8422 ± 10	8688 ± 10	$1.27^{+0.63}_{-0.31}$
133.0 ± 0.1 ($K_{\beta 1}$(Es))	–	–	–
138.1 ± 0.3	8403 ± 10	8679 ± 10	$0.77^{+0.62}_{-0.24}$
157.1 ± 0.1	(8455 ± 2)	–	$1.08^{+0.20}_{-0.15}$
164.0 ± 0.7	8408 ± 9	8710 ± 9	$1.44^{+1.00}_{-0.42}$
209.6 ± 0.1	8421 ± 1	8769 ± 1	1.08 ± 0.31
219.0 ± 0.1	8421 ± 13	8779 ± 13	$0.95^{+0.95}_{-0.32}$
271.4 ± 1.5	8371 ± 13	8780 ± 13	–
294.0 ± 0.3	8334 ± 11	8765 ± 11	–
342.1 ± 1.3	8451 ± 11	8932 ± 11	$0.36^{+0.27}_{-0.15}$
352.2 ± 0.7	(8351)	–	–

the theoretical value of 0.651. The reason for this deviation is unclear, as on the other side the intensity ratio $I_{K\beta 1}/I_{K\alpha 2} = 0.36 \pm 0.12$ is in-line with the theoretical value of 0.372.

E_γ = 219.0 keV-line The half-life of the coincident α decays of 0.95 s and their energy of 8421 keV suggest that the 219.0-keV line is emitted from the same state as the 209.6 keV line but populating a level 9.5 keV lower. The transition rate, however, is considerably smaller for the 219.0-keV transition. We obtained an intensity ratio $I(219.0)/I(209.0) = 0.023 \pm 0.002$, which suggests that this line has no E1 multipolarity, but rather M1 or E2. Higher multipolarities can be excluded as for those cases the expected half-lives are $\gg 10\,\mu$s and thus the γ events would not have been observed within the $5\,\mu$s coincidence window of the data acquisition system.

E_γ = 114.4 keV-line The half-life of 1.87 s suggests an assignment to the decay of ^{247g}Md; the broad α-particle energy distribution is probably due to energy summing with conversion electrons (CE). On the basis of the present data no safe assignment to a level in ^{243}Es can be made.

E_γ = 126.9 keV-line This line was observed in coincidence with α decays of $E_\alpha = (8422 \pm 10)$ keV. This energy suggests the emission of the 126.9-keV line from the same level as the $E_\gamma = 209.6$ keV line.

E_γ = 138.1 keV and E_γ = 164.0 keV-lines The very similar mean energies of the coincident alpha particles suggest decay into the same level. The mean energy of the coincident α particles (8406 keV) on the other hand is 15 keV lower as for those coincident with the 209.6 keV line, suggesting to originate from a different level. A mean half-life of 1.27 s is obtained from all α-γ(138.1, 164.0 keV), which suggests an assignment to the decay of ^{247g}Md.

E_γ = 270.1 keV and E_γ = 272.1 keV-lines The broad distribution of the γ energies in that region suggests a line doublet, but the very similar α energies the emission from the same level. Taking the mean value for γ and α energies we obtain $E_\gamma = 271.4 \pm 1.5$ keV and $E_\alpha = 8371 \pm 13$ keV and hence a Q value of 8779 ± 16 keV, which agrees with the value 8779 ± 13 keV for the 219.0-keV transition. Thus we tentatively regard that somewhat broader distribution as a single transition populating the same level as the 219.0 keV transition.

E_γ = 294.0 keV-line This weak line is in coincidence with α particles of $E_\alpha = 8334 \pm 11$ keV. The Q value of 8765 ± 11 keV is, although being within the error bars, significantly lower than the values for the 219.0 and 271.4 keV transitions, but agrees rather well with the value $Q = 8769 \pm 1$ keV for the $E_\gamma = 209.6$ keV transition. So tentatively we prefer to assign it to a decay into the same level as the 209.6 keV transition.

E_γ = 342.1 keV-line Although the α energies are in the range of those in coincidence with the 157.1, 209.6, and 219.0 keV transitions the half-life of 0.36 s is definitely shorter than that of ^{247g}Md, and within the error bars it is in agreement with that of ^{247m}Md. The broad distribution of the α energies suggests two lines of $E_\alpha = 8402 \pm 5$ keV and $E_\alpha = 8451 \pm 11$ keV and the population of two levels by α decay, but tentatively we interprete the γ events as being emitted from the same level, i.e. the lower one.

E_γ = 352.7 keV-line This line seems somewhat questionable; one event was in coincidence with an α particle of $E_\alpha = 8351$ keV and four events with α particles of $E_\alpha = (8670–8962)$ keV. For these cases the sum energy $E_\gamma + E_\alpha$ exceeds the maximum α energies or α-γ sum energies for ^{247g}Md and ^{247m}Md considerably. So an assignment to ^{247}Md decay is not straightforward.

4 Discussion

4.1 Decay of ^{247g}Md

The proposed decay scheme is shown in Fig. 4. In addition to the assignment of the previously reported lines (209.6, 157.1 keV) we also assign, based on the same energy of the coincident α particles as for the 209.6 keV transition, the line at 219.0 keV as a transition from the $7/2^-$ level. But due to the higher Q value it populates a level 9.5 keV lower in excitation energy, which we assign as the ground-state in ^{243}Es and, tentatively, as the $3/2^-[521]$ Nilsson level. This is in-line with the possible E2 multipolarity of the 219.0-keV transition.

Assignments of the other γ transitions attributed to the decay of ^{247}Md are more speculative.

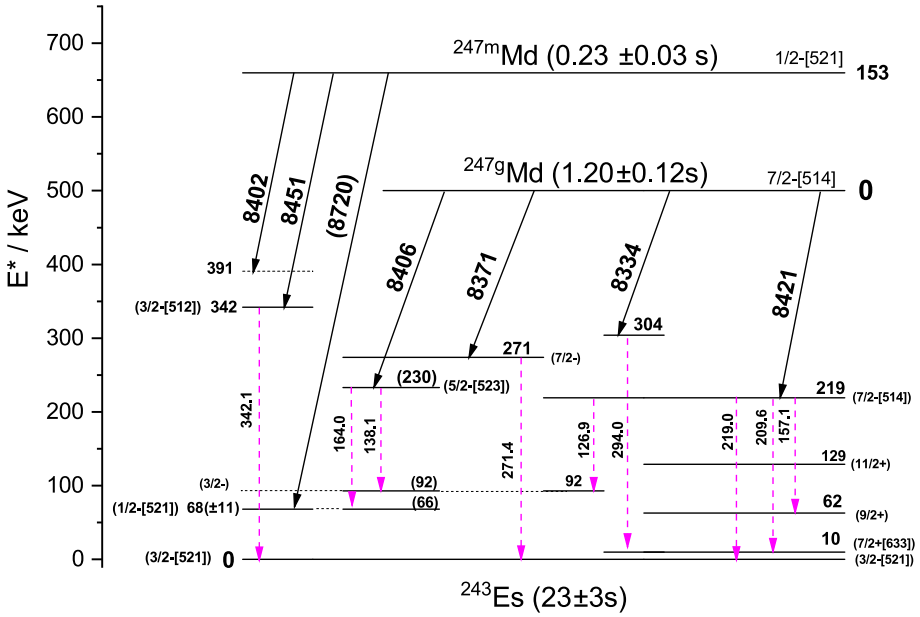

Fig. 4 Proposed tentative decay scheme of ^{247}Md. Half-lives for ^{247g,247m}Md are from this work, half-life of ^{243}Es is taken from [9]. α transitions are represented by full lines, γ transitions by dashed lines

The energy sum $E_\alpha + E_\gamma = 8371$ keV + 271 keV = 8642 keV ($Q = 8779 \pm 16$ keV) is practically equal to $E_\alpha + E_\gamma = 8421$ keV + 219 keV = 8640 keV ($Q = 8779 \pm 13$ keV), so we attribute it also to a decay into the ground-state of ^{243}Es. As the γ events are observed in prompt coincidence with α decays, the lifetime of the level must be $<1\,\mu$s, thus the multipolarity is restricted to E1, E2 or M1. Conversion coefficients for transitions of 271 keV are $\alpha = 0.0581$ (E1), 0.0409 (E2), 2.48 (M1) [19]. Using the number of observed γ events (three events between the beam bursts with full α-energy release in the stop detector), an efficiency of the clover detector of $\epsilon = 0.12$, the total number of α events and the half-life of ^{247g}Md given in Table 1, we obtain partial α half-lives $T_\alpha = 47$–157 s. The calculated α half-life is $T_\alpha(\text{calc}) = 1.6$ s. Hence, one obtains hindrance factors HF = 30–100. These values hint to an α transition without parity change and without a spin flip [20]. Under these considerations and taking into account that the $3/2^-[521]$ level is assumed to be the final state, among the Nilsson levels predicted at $E^* \leq 1000$ keV [21], the $5/2^-[523]$-state or the first excited level $(7/2^-)$ of the rotational band built up on it are the best choices.

The energy difference of the α particles in coincidence with the γ transitions $E_\gamma = 138.1$ keV ($E_\alpha = 8403$ keV) and $E_\gamma = 164.0$ keV ($E_\alpha = 8408$ keV) is only 5 keV. Due to this small value and the overlapping error bars we assign them to the decay into the same level with an α-decay energy of 8406 ± 10 keV (mean value for α decays in coincidence with both γ transitions). The assingment of the level populated by this transition is under discussion. On the basis of the α energy it can be located $\approx$15 keV above the $7/2^-[514]$ level, i.e. at $E^* = 234$ keV. The levels populated by the 164.0-keV and 138.1-keV transitions are then located at $E^* = 70$ keV and $E^* = 96$ keV. On the other side, the $E_\gamma = 126.9$ keV is assumed on the basis of the coincident α energy to depopulate the level at 219 keV, thus populating a level at $E^* = 92$ keV. Due to the small energy difference of 4 keV, we tentatively assign both transtions to populate the same level, which we locate at $E^* = 92$ keV, due to the more precise α energy for the transition populating the $E^* = 219$ keV level. The energy of the level populated by the 164.0 keV is then $E^* = 66$ keV, the energy of the emitting level is thus $E^* = 230$ keV as shown in Fig. 4. As the level energies are derived of the decay $E_\alpha = 8421$ keV, $E_\gamma = 126.9$ keV as discussed above, the level energies are given in brackets.

4.2 Decay of ^{247m}Md

The isomeric state was already earlier tentatively assigned as $1/2^-[521]$ since the relatively long half-life of 0.23 s requires an angular momtentum difference of $\Delta l \geq 3$ to lower-lying states and thus it is the only candidate as long as the ground-state is assigned as $7/2^-[514]$. The calculated α-decay half-life for $E_\alpha = 8780$ keV is $T_\alpha = 0.1$ s [15,16] resulting in HF = 3.6: thus it is seemingly an unhindered transition between states of the same configuration ($1/2^-[521]$) in the mother and the daughter nucleus.

The 342.1 keV line is in coincidence with α decays of $T_{1/2} = 0.36$ s, therefore it is attributed to the decay of the isomeric state. On the basis of five γ events and a calculated α-decay half-life of $T_\alpha = 0.39$ s a hindrance factor $\approx$7 for both, the $E_\alpha = 8451$ keV, and the $E_\alpha = 8402$ keV activities is obtained on the basis of 0.23 s half-life of the isomeric state and the equal intensity for both transitions. The low hindrance factor indicates that mother and daughter states have a similar structure. A possible Nilsson level in question is the $3/2^-[512]$, however, such a level is not predicted in ^{243}Es at excitation energies below 1 MeV [21]. The only level predicted below 1 MeV excitation energy and so far not

(tentatively) assigned is the $5/2^+[642]$ level which would require a parity change. Therefore a decay in that level is not in-line with the low hindrannce factor, we tentatively assign $3/2^-[512]$ to the level populated by the α decay.

On that basis the 342.1 keV transition is tentatively attributed to the decay into the ground state, as e.g. decay into the $7/2^+[633]$ would require an M2 transition having a life-time $>1\mu$s. Thus the γ events would not have been observed in prompt coincidence with the α particles. The resulting Q value is 8932 ± 10 keV and the energy difference to the $E_\alpha = 8780$ keV transition ($Q = 8924$ keV) is $\Delta E \approx 8$ keV. Although the energy difference is low and within the error bars of the energy of the α particles in coincidence with the 342.1 keV γ transitions, α decay (8780 keV) into the $3/2^-[521]$ level can be excluded as it requires a spin flip and thus is strongly hindered (HF $>$ 1000). Therefore the difference is explained by feeding an excited state, assigned as $1/2^-$ on the basis of the low α decay hindrance factor as discussed above, decaying predominantly by internal conversion as expected for the M1 transition $1/2^-[521] \rightarrow 3/2^-[521]$ with the measured α energy (apparent energy) representing the sum of the α-decay energy and the conversion electron energy. In such a case the excitation energy of the $1/2^-[521]$ state cannot be simply taken from the energy balance.

To obtain an estimate for the excitation energy of the $1/2^-[521]$ level we performed GEANT 4 simulations [22]. Calculations were performed assuming an M1 transition and a total decay Q value of 8932 keV for excitation energies in the range $E^* = (35–80)$ keV. A certain contribution from the deexcitation of the atomic shell (Auger electrons, soft X-rays) to the energy summing was respected. We took a value of $E = 0.6 \times E_B$, with E_B being the average L-binding energy of einsteinium. The factor 0.6 was obtained from an analysis of the energy summing of CE and ^{253}No α decays in coincidence with 221.5 keV γ transitions populating the $9/2^+$ level in ^{249}Fm at $E^* = 58.3$ keV [23]. Best representation of the experimental data was obtained for $E^* = 65$ keV and $E^* = 70$ keV (see Fig. 5a, b), where the experimental (full lines) and simulated (dashed lines) α-energy distributions are shown.

As a measure for the agreement betwen experimental results and simulations we took the square of the differences between the number of experimental α decays (z_{exp}) within an energy bin of 5 keV, and the number of simulated events (z_{sim}) divided by the number N of respected bins

$$X^2 = \Sigma(z_{exp} - z_{sim})^2/N$$

The total number of simulated events was normalized to the total number of observed events. The result of comparing experimental data and simulations, i.e. this X^2 analysis, is shown in Fig. 5c. Fitting the data by a polynom of fourth order (dashed line in Fig. 5c), we obtain the minimum deviation at $E^* = 68 \pm 2$ keV. Respecting the uncertainty of the Q value ($Q = 8931 \pm 11$ keV), the $1/2^-[521]$ level is settled at $E^* = 68 \pm 11$ keV.

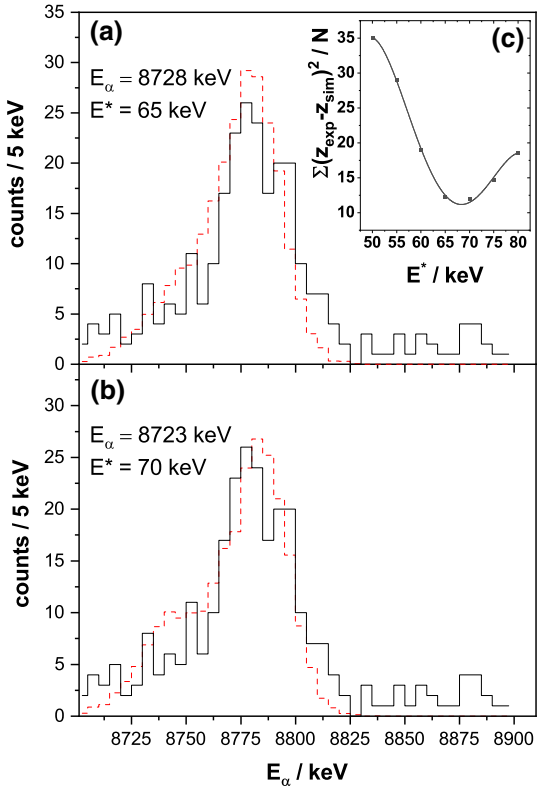

Fig. 5 Comparison of observed and simulated α spectrum of ^{247m}Md; **a** simulation using $E^* = 65$ keV and $E_\alpha = 8728$ keV; **b** simulation with $E^* = 70$ keV and $E_\alpha = 8723$ keV. The concentration of α events in the energy range $E = (8850–8900)$ keV ist due to ^{211m}Po (8883 keV) produced by pn-transfer from the target nucleus ^{209}Bi. **c** X^2 distribution for Q^* (50–80) keV

The location of the $1/2^-[521]$ state at $E^* = 68$ keV has some consequences for the assignment of the levels populated by the 164.0 and 138.1 keV transitions. Candidates populated by the 164.0-keV transtion are: the $9/2^+$ level of the rotational band built up on the $7/2^+[633]$ Nilsson state, the $7/2^-$ level of the rotational band built up on the $3/2^-[521]$ Nilsson state, and the $1/2^-[521]$ Nilsson state. The $9/2^+$ state is located at $E^* = 62$ keV (see Fig. 4) and is not considered further. Energy differences between the $3/2^-[521]$ state and the $7/2^-$ member of the rotational band, when known, are 75 ± 3 keV in einsteinium and berkelium isotopes [18]. Although the lower value of 66 keV suggests a different level, with respect to the error bar of the corresponding α energy this level cannot be ruled out completely. The best choice, however, seems the $1/2^-[521]$ Nilsson state. This assignment is supported by the energy difference of 25.9 keV between the 164.0 and 138.1 keV γ lines, a value which is in typical range (20 - 30 keV) for 1/2 and 3/2 states of a rotational band in the transuranium region [18]. As the multipolarity of

both γ transitions is restricted to E1, E2 or M1 (transitions of other multipolarities would not be observed in prompt coincidence with α particles due to half-lives $\gg 1\mu$) the $5/2^-[523]$ - Nilsson state, predicted at ≈850 keV [21] and at 390 keV [24] seems to be a good candidate for the emitting level. The level depopulated by the 271.4-keV transition may then be assigned as the $7/2^-$ state of the rotational band built up on $5/2^-[523]$.

4.3 Comparison of predicted and experimentally assigned levels

In Fig. 6 we compare experimental levels as derived from this work with theoretically predicted ones. Fig. 6a shows the results from a Hartree–Fock–Bogoliubov (HFB) calculation using the SLy4 parametrization [6], Fig. 6b, c display the results from macroscopic–microscopic (MM) calculations from Parkhomenko et al. [21] (Fig. 6b) and from Adamian et al. [24] (Fig. 6c), while the experimental values as extracted from this work are shown in Fig. 6d. Evidently theoretical calculations do not reproduce the $3/2^-[521]$ as ground-state, the MM-caculations predict $7/2^+[633]$ [21,24] as ground-state, while the HFB calculations predict $1/2^-[521]$ [6]. Experimentally that state was located at 68 keV in our experiment; MM calculations of [21] predict it at ≈400 keV, while in [24] it is not among the levels predicted below 500 keV. The $7/2^-[514]$ and the $5/2^-[523]$ states are observed at lower energies than predicted by all calculations [6,21,24]. Also the experimental level energy values exhibit a stronger compression of the levels in energy than the calculated ones. A detailed discussion of this discrepancies requires enhanced theoretical calculations, which are beyond the scope of this study. Therefore we will do here with some qualitative discussion, which may serve as a guide for further theoretical work. The levels considered here, except the $5/2^-[523]$ which is therefore disregared in the further discussions, stem from nuclear subshells relevant for the shell gap expected at $Z = 114$ from macroscopic-microscopic calculations [25,26] or at $Z = 120$ for some of the Hartee–Fock–Bogoliubov (as e.g. the SLy4 parametrization) and Relativistic Meanfield calculations (see e.g. [27]), specifically:
$1h_{9/2} \rightarrow 7/2^-[514]$
$1i_{13/2} \rightarrow 7/2^+[633]$
$2f_{7/2} \rightarrow 3/2^-[521]$
$2f_{5/2} \rightarrow 1/2^-[521]$
$1h_{9/2} \rightarrow 5/2^-[523]$.

The $1h_{9/2}$, $1i_{13/2}$ and $2f_{7/2}$ subshells are located below the shell gap at Z=114, the $2f_{5/2}$ subshell above it [28]. From the Nilsson diagram [28] one obtains a Nilsson level ordering $3/2^-[521]$, $7/2^+[633]$, $7/2-[514]$, $1/2^-[521]$ at a quadrupole parameter $\beta_2 = 0.224$ for ^{243}Es [26] as shown in Fig. 6e. Evidently the level energies of the $3/2^-[521]$, $7/2^+[633]$, $7/2-[514]$ are not in a striking disagreement with the single–particle energies from the Nilsson diagram, considering the 'simple model' they are based on, while it is striking for the $1/2^-[521]$ level. As a reason for this behavior one could imagine a steeper decrease of the $1/2^-[521]$ level with deformation or a smaller energy difference of the $2f_{7/2}$ and $2f_{5/2}$ spin-orbit partners. The latter would be of high interest as it was stressed in [27] that:

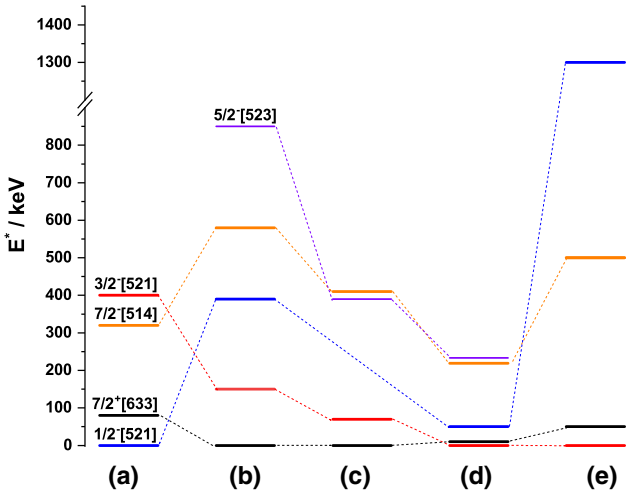

Fig. 6 Comparison of calculated **a** [6], **b** [21], **c** [24] and **d** experimental low lying levels in ^{243}Es; **e** shows the sequence in the Nilsson diagram in Ref. [28]. Please note: data in **a** are taken from Fig. 15 in [6] and are thus approximate; data in **e** are from Fig. 4 in [28] and represent the single-particle energies at quadrupole deformation ν_2=0 with the energy for the $3/2^-[521]$ level arbitrarily set to $E = 0$ for better presentation; energy values are also approximate

(a) the strength of the spin-orbit interaction is an uncertain ingredient in theoretical calculations
(b) the energy difference between the $2f_{7/2}$ and $2f_{5/2}$ proton single-particle levels defines whether the spherical shell gap in the region of superheavy elements occurs at $Z = 114$ or $Z = 120$.

Thus the low excitation energy of the $1/2^-[521]$ level could be a hint that the spherical proton shell may rather be located at $Z = 120$ than at $Z = 114$. It should be noted in this context that in a recent decay study of ^{286}Fl [29] the authors came to a similar conclusion, stating that the next proton shell closure beyond ^{208}Pb ($Z = 82$) would not be located at $Z = 114$.

4.4 Spontaneous fission hindrance of ^{247g}Md and ^{247g}Md

It is well known that spontaneous fission of odd-mass nuclei is hindered compared to their neighbouring even-even isotopes. Qualitatively fission hindrance can be expressed by a hindrance factor $HF = T_{SF}/T_{SF}(\text{ee})$ with T_{SF} being the experimental fission half-life and $T_{SF}(\text{ee})$ being see 'unhindered'

fission half-life represented by the geometrical mean of the neighboring even–even nuclei (see e.g. [30]). In the case of ^{247}Md these nuclei are ^{246}Fm and ^{248}No. As the latter nuclide has not been identified so far, no experimental 'absolute' fission hindrance factor can be given, but on the basis of the measured fission half-lives a 'relative' hindrance between the ground-state and the isomeric state. Fission branches $b_{sf} = 0.0086 \pm 0.0010$ for ^{247g}Md and $b_{sf} = 0.20 \pm 0.02$ for ^{247m}Md were determined and spontaneous fission half-lives of ≈140 s and ≈1.2s were obtained for ^{247g}Md and ^{247m}Md in our experiment. Thus spontaneous fission of the high-spin ground state ($7/2^-[514]$) is hindered by a factor of ≈120 stronger than that of the low-spin isomeric state ($1/2^-[521]$). The energy of the Nilsson level $7/2^-[514]$ increases at deformation, while that of the $1/2^-[521]$ Nilsson level decreases [28]. This finding supports the conclusion of a tendency of higher fission probabilities of Nilsson levels downsloping in energy at increasing deformation [30].

5 Conclusion

The decay of ^{247}Md was investigated by α-γ spectroscopy; four low lying Nilsson levels in the daughter nucleus ^{243}Es were identified, the ground-state was assigned as $3/2^-[521]$.

An excitation energy of 153 keV was measured for the 0.231 s isomeric state in ^{247}Md. The low energy difference 68 ± 11 keV of $3/2^-[521]$ and $1/2^-[521]$ Nilsson levels in the daughter nucleus ^{243}Es stemming from the $2f_{7/2}$ and $2f_{5/2}$ spin-orbit partners, could be a hint that these two levels are closer in energy and thus the spherical proton shell is rather located at $Z = 120$ than at $Z = 114$.

Acknowledgements We thank the UNILAC staff as well as the ion source crew for delivering beams of high and stable intensity. We are also grateful to J. Steiner, B. Lommel and B. Kindler for production of the large area targets. We want to express our gratitude to H.G. Burkhard and J. Maurer for skillful maintenance of the mechanical and electrical components of SHIP and S. Hofmann for his support in preparing the experiment. The work has been supported by the Slovak Research and Development Agency (contract No. APVV-18-0268 and APVV-20-0532) and Scientific Grant Agency VEGA (Contract No. 1/0651/21 and contract nr. 2/0067/21).

Funding Open Access funding enabled and organized by Projekt DEAL.

Data Availability Statement This manuscript has no associated data or the data will not be deposited. [Author's comment: All data generated during this study are contained in this published article.]

References

1. S.G. Nilsson, C.F. Tsang, A. Sobiczewski, Z. Szymanski, S. Wycech, C. Gustafson, I.-L. Lamm, P. Möller, B. Nilsson, Nucl. Phys. A **131**, 1 (1969)
2. M. Asai, F.P. Heßberger, A. Lopez-Martens, Nucl. Phys. A **944**, 308 (2017)
3. D. Ackermann, Ch. Theisen, Phys. Scr. **92**, 083002 (2015)
4. I. Ahmad, R.R. Chasman, P.R. Fields, Phys. Rev. C **61**, 044301 (2000)
5. F.P. Heßberger, S. Antalic, B. Streicher, S. Hofmann, D. Ackermann, B. Kindler, I. Kojouharov, P. Kuusiniemi, M. Leino, B. Lommel, R. Mann, K. Nishio, S. Saro, B. Sulignano, Eur. Phys. J. A **26**, 233 (2005)
6. A. Chatillon, Ch. Theisen, P.T. Greenlees, G. Auger, J.E. Bastin, E. Bouchez, B. Bouriquet, J.M. Casandjian, R. Cee, E. Clement, R. Dayras, G. de France, R. de Toureil, S. Eeckhaudt, A. Görgen, T. Grahn, S. Grevy, K. Hauschild, R.-D. Herzberg, P.J.C. Ikin, G.D. Jones, P. Jones, R. Julin, S. Juutinen, H. Kettunen, A. Korichi, W. Korten, Y. LeCoz, M. Leino, A. Lopez-Martens, S.M. Lukyanov, Yu.E. Penionzkhevich, J. Perkowski, A. Pritchard, P. Rahkila, M. Rejmund, J. Saren, C. Scholey, S. Siem, M.G. Saint-Laurent, C. Simenel, Yu.G. Sobolev, Ch. Stodel, J. Uusitalo, A. Villari, M. Bender, P. Bonche, P.-H. Heenen, Eur. Phys. J. A **30**, 397 (2006)
7. I. Ahmad, R.K. Sjoblom, R.F. Barnes, E.P. Horwitz, P.R. Fields, Nucl. Phys. A **140**, 141 (1970)
8. K. Moody, R.W. Lougheed, J.F. Wild, R.J. Dongan, E.K. Hulet, R.W. Huff, C.M. Henderson, R.J. Dupzyk, K. Sümmerer, G.D. O'Kelly, G.R. Bertune, Nucl. Phys. A **563**, 21 (1993)
9. S. Antalic, F.P. Heßberger, S. Hofmann, D. Ackermann, S. Heinz, B. Kindler, I. Kojouharov, P. Kuusiniemi, M. Leino, B. Lommel, R. Mann, S. Saro, Eur. Phys. J A **43**, 35 (2010)
10. G. Münzenberg, S. Hofmann, W. Faust, F.P. Heßberger, W. Reisdorf, K.-H. Schmidt, T. Kitahara, P. Armbruster, K. Güttner, B. Thuma, D. Vermeulen, Z. Phys. A **302**, 7 (1981)
11. S. Hofmann, V. Ninov, F.P. Heßberger, H. Folger, G. Münzenberg, H.J. Schött, P. Armbruster, A.N. Andreyev, A.G. Popeko, A.V. Yeremin, M.E. Leino, R. Janik, S. Saro, M. Veselsky, GSI Scientific Report 1993 (FSI 04-1), 64 (1994)
12. G. Münzenberg, W. Faust, S. Hofmann, P. Armbruster, K. Güttner, H. Ewald, Nucl. Instr. Methods **161**, 65 (1979)
13. S. Hofmann, D. Ackermann, S. Antalic, H.G. Burkhard, V.F. Comas, R. Dressler, Z. Gan, S. Heinz, J.A. Heredia, F.P. Heßberger, J. Khuyagbaatar, B. Kindler, I. Kojouharov, P. Kuusiniemi, M. Leino, B. Lommel, R. Mann, G. Münzenberg, K. Nishio, A.G. Popeko, S. Saro, H.J. Schött, B. Streicher, B. Sulignano, J. Uusitalo, M. Venhart, A.V. Yeremin, Eur. Phys. J. A **32**, 251 (2007)
14. M. Venhart, F.P. Heßberger, D. Ackermann, S. Antalic, C. Gray-Jones, P.T. Greenlees, S. Heinz, R.-D. Herzberg, S. Hofmann, S. Ketelhut, B. Kindler, I. Kojouharov, M. Leino, B. Lommel, R. Mann, P. Papadakis, D. Rostron, D. Rudolph, S. Saro, Eur. Phys. J. A **47**, 20 (2011)
15. D.N. Poenaru, M. Ivascu, D. Mazilu, J. Phys. Lett. **47**(20), 589 (1980)
16. E. Rurarz, Acta Phys. Pol. B **14**, 917 (1983)

17. F.P. Heßberger, S. Antalic, D. Ackermann, B. Andel, M. Block, Z. Kalaninova, B. Kindler, I. Kojoiharov, M. Laatiaoui, B. Lommel, K. Mistry, J. Piot, M. Vostinar, Eur. Phys. J. A **52**, 328 (2016)
18. R.B. Firestone, V.S. Shirley, S.Y. Chu, C.M. Bagkin, J. Zipkin (eds.), *Table of Isotopes*, 8th edn. (John Wiley & Sons, New York, 1996)
19. T. Kibeti, T.W. Burrows, M.B. Trzhaskovskaya, P.M. Davidson, C.W. Nestor Jr., Nucl. Instr. Meth. A **589**, 202 (2008)
20. G.T. Seaborg, W. Loveland, *The Elements Beyond Uranium* (John Wiley & Sons Inc, New York, 1990), p. 153
21. A. Parkhomenko, A. Sobiczewski, Acta Phys. Pol. B **35**, 2447 (2004)
22. S. Agostinelli, J. Allison, K. Amako, J. Apostolakis, H. Ataujo, P. Arce, M. Asai, D. Axen, S. Banerjee, G. Barrand, F. Behner, L. Bellagamba, J. Boudreau, L. Briglia, A. Brunengo, H. Burkhardt, S. Chauvie, J. Chuma, R. Chytracek, G. Cooperman, G. Cosmo, P. Degtyarenko, A. Dell'Acqua, G. Pepaola, D. Dietrich, R. Enami, A. Feliciello, C. Ferguson, H. Fesefeldt, G,. Folger, F. Foppiano, A. Forti, S. Garelli, S. Giani, R. Giannitrapani, D. Gibin, J.J. Gomez Cadenas, I. Gonzalez, G. Gracia April, G. Greeniaus, W. Greiner, V. Grichine, A. Grossheim, S. Guatelli, P. Gumplinger, R. Hamamatsu, K. Hashimoto, H. Hasui, A. Heikkinen, A. Howard, V. Ivanchenko, A. Johnson, F.W. Jones, J. Kallenbach, N. Kanaya, M. Kawabata, Y. Kawabata, M. Kawaguti, S. Kelner, P. Kent, A. Kimura, T. Kodama, R. Kokoulin, M. Kossov, H. Kurashinge, E. Lamanna, T. Lampen, V. Lara, V. Lefebure, F. Lei, M. Liendl, W. Lockman, F. Longo, S. Magni, M. Maire, E. Medernach, K. Minamimoto, P. Mora de Freitas, Y. Morita, K. Murakami, M. Nagamatu, R. Nartallo, P. Nieminen, T. Nishimura, K. Ohtsubo, M. Okamura, S. O'Neale, Y. Oohata, K. Paech, J. Perl, A. Pfeiffer, M.G. Pia, F. Ranjard, A. Rybin, S. Sadilov, E. Di Salvo, G. Santin, T. Sasaki, N. Savvas, Y. Sawada, S. Scherer, S. Sei, V. Sirotenko, D. Smith, N. Starkov, H. Stoecker, J. Sulkimo, M. Takahata, S. Tanaka, E. Tcherniaev, E. Safai Tehrani, M. Tropeano, P. Truscott, H. Uno, L. Urban, P. Urban, M. Verderi, A. Walkden, W. Wander, H. Weber, J.P. Wellisch, T. Wenaus, D.C. Williams, D. Wright, T. Yamada, H. Yoshida, D. Zschiesche, Nucl. Instr. Meth. Phys. Res. A **506**, 250 (2003)
23. F.P. Heßberger, S. Antalic, D. Ackermann, Z. Kalaninova, S. Heinz, S. Hofmann, B. Streicher, B. Kindler, I. Kojouharov, P. Kuusiniemi, M. Leino, B. Lommel, R. Mann, K. Nishio, S. Saro, B. Sulignano, M. Venhart, Eur. Phys. J. A **48**, 75 (2012)
24. G.G. Adamian, N.V. Antonenko, S.N. Kaklin, W. Scheid, Phys. Rev. **82**, 054304 (2010)
25. R. Smolanczuk, A. Sobiczewski, in Proc. EPS Conf. 'Low Energy Nuclear Dynamics', ed. by St. Petersburg, Yu. Ts. Oganessian et al. (World Scientific, Singapore, New Jersey, London, Hong Kong, 1995), p. 313
26. P. Möller et al., Atom. Data Nucl. Data Tables **59**, 185 (1995)
27. M. Bender, K. Rutz, P.-G. Reinhard, J.A. Maruhn, W. Greiner, Phys. Rev. C **60**, 034304 (1999)
28. R.R. Chasman, I. Ahmad, A.M. Friedman, J.R. Erskine, Rev. Mod. Phys. **49**, 833 (1977)
29. A. Samark-Roth, D.M. Cox, D. Rudolph, L.G. Sarmiento, B.G. Carlsson, J.L. Egido, P. Golubev, J. Heery, A. Yakushev, S. Aberg, H.M. Albers, M. Albertsson, M. Block, H. Brand, T. Calverley, R. Cantemir, R.M. Clark, Ch.E, Düllmann, J. Eberth, C. Fahlander, U. Forsberg, J.M. Gates, F. Giacoppo, M. Götz, S. Götz, R.-D. Herzberg, Y. Hrabar, E. Jäger, D. Judson, J. Khuyagbaatar, B. Kindler, I. Kojouharov, J.V. Kratz, J. Krier, N. Kurz, L. Lens, J. Ljungberg, B. Lommel, J. Louko, C-.C. Meyer, A. Mistry, C. Mokry, P. Papadakis, E. Parr, J.L. Pore, I. Ragnarsson, J. Runke, M. Schädel, H. Schaffner, B. Schausten, D.A. Shaughnessy, P. Thörle - Pospiech, N. Trautmann, J. Uusitalo, Phys. Rev. Lett. **126**, 032503 (2021)
30. F.P. Heßberger, Eur. Phys. J. A **53**, 75 (2017)